Interactions of subunit CCT3 in the yeast chaperonin CCT/TRiC with Q/N-rich proteins revealed by high-throughput microscopy analysis

Michal Nadler-Holly[a,1], Michal Breker[b,1], Ranit Gruber[a], Ariel Azia[a,c], Melissa Gymrek[d], Miriam Eisenstein[e], Keith R. Willison[f], Maya Schuldiner[b,2], and Amnon Horovitz[a,2]

Departments of [a]Structural Biology, [b]Molecular Genetics, and [e]Chemical Research Support, Weizmann Institute of Science, Rehovot 76100, Israel; [c]The Mina and Everard Goodman Faculty of Life Sciences, Bar-Ilan University, Ramat-Gan 52900, Israel; [d]Whitehead Institute for Biomedical Research, Cambridge, MA 02142; and [f]Department of Chemistry, Institute of Chemical Biology, Imperial College London, London SW7 2AZ, United Kingdom

Edited* by George H. Lorimer, University of Maryland, College Park, MD, and approved October 2, 2012 (received for review June 12, 2012)

The eukaryotic chaperonin containing t-complex polypeptide 1 (CCT/TRiC) is an ATP-fueled machine that assists protein folding. It consists of two back-to-back stacked rings formed by eight different subunits that are arranged in a fixed permutation. The different subunits of CCT are believed to possess unique substrate binding specificities that are still mostly unknown. Here, we used high-throughput microscopy analysis of yeast cells to determine changes in protein levels and localization as a result of a Glu to Asp mutation in the ATP binding site of subunits 3 (CCT3) or 6 (CCT6). The mutation in subunit CCT3 was found to induce cytoplasmic foci termed P-bodies where mRNAs, which are not translated, accumulate and can be degraded. Analysis of the changes in protein levels and structural modeling indicate that P-body formation in cells with the mutation in CCT3 is linked to the specific interaction of this subunit with Gln/Asn-rich segments that are enriched in many P-body proteins. An in vitro gel-shift analysis was used to show that the mutation in subunit CCT3 interferes with the ability of CCT to bind a Gln/Asn-rich protein aggregate. More generally, the strategy used in this work can be used to unravel the substrate specificities of other chaperone systems.

molecular chaperones | polyQ proteins | protein mis-folding | protein aggregation | high-content analysis

Chaperonins are ATP-dependent protein-folding machines that are present in all kingdoms of life. They consist of two back-to-back stacked oligomeric rings with a cavity at each end, where protein substrate binding and folding take place (for reviews see refs. 1 and 2). The chaperonins can be divided into two groups: group I, found in the bacterial cytoplasm (e.g., GroEL in *Escherichia coli*), mitochondria, and chloroplasts; and group II found in archaea and the eukaryotic cytosol. Numerous studies have shown that the group I chaperonin GroEL can facilitate the folding of a large number of different proteins in vitro, although its role in the cell is much more limited (for review see ref. 3). The group II eukaryotic chaperonin containing t-complex polypeptide 1 (CCT/TRiC) also seems to have a specialized role in vivo in the folding of actin (4), tubulin (5), and other essential proteins, including regulators of cell division and cytoskeleton formation (6–8), despite seeming to possess broad binding specificity (6). The list of members in the CCT interactome is, however, not yet fully established, and the conditions for entry into this exclusive club remain poorly understood.

An important distinction between group I and group II chaperonins is that the former consist of homo-oligomeric rings, whereas the latter usually consist of hetero-oligomeric rings that contain two or three different subunits in the case of many archaeal chaperonins and eight different subunits in the case of CCT. The eight subunits of CCT are arranged in a defined permutation (9), and the orientation of the two rings of CCT with respect to each other is also fixed (10). CCT's hetero-oligomeric structure has enabled a combinatorial mode of protein substrate binding to specific subunits (8, 11) to coevolve as found in the case of actin, for example, which binds to particular subunits on both sides of the ring (11). Hence, additional challenges, in the case of CCT, are (*i*) to characterize the (potentially overlapping) interactomes of different combinations of subunits and (*ii*) to establish which properties of a substrate determine its dependence on a specific subset of CCT subunits for efficient folding. The hetero-oligomeric structure of CCT is also most likely responsible for its sequential intraring allostery (12) that differs from the concerted mechanism of GroEL (13). It has been suggested that sequential allostery facilitates domain-by-domain substrate release in a temporal order that is determined by the specific subunits to which the substrate is bound (12).

To obtain further insight into the functional significance of CCT's hetero-oligomeric structure, we recently generated (14) a set of *Saccharomyces cerevisiae* yeast strains in which an aspartic acid, which is conserved in the ATP binding site of all eight subunits (and also across species), is mutated to glutamic acid in each subunit of CCT in turn. In vivo analyses of these CCT mutant yeast strains revealed surprisingly large phenotypic differences between them in, for example, growth rates, heat and cold sensitivities, and morphologies. The phenotypic differences between the strains are likely to be due, in part, to misfolding of substrates that require the mutated subunit for efficient folding (Fig. 1*A*). These yeast strains, therefore, provide an excellent model system for gaining insight into the substrate specificities of the different subunits. Here we describe progress in this direction that was attained by high-throughput microscopy screening (15, 16) of a library generated by crossing strains with a mutation in CCT3 or CCT6 with a library of strains expressing different yeast ORFs fused to GFP (17) (Fig. 1*B*). Our results show that each of the mutations in CCT produced a unique effect on the yeast proteome and, more specifically, that subunit CCT3 has a stronger interaction in vivo with Q/N-rich proteins than subunit CCT6. In particular, subunit CCT3 is found to interact with Q/N-rich proteins that form cytoplasmic foci termed P-bodies, where mRNAs that are not being translated accumulate and can be degraded (18). More broadly, our results demonstrate that unraveling

Author contributions: M.N.-H., M.B., M.S., and A.H. designed research; M.N.-H., M.B., R.G., M.E., K.R.W., and A.H. performed research; M.N.-H., M.B., R.G., A.A., M.G., K.R.W., M.S., and A.H. analyzed data; and M.S. and A.H. wrote the paper.

The authors declare no conflict of interest.

*This Direct Submission article had a prearranged editor.

Freely available online through the PNAS open access option.

[1]M.N.-H. and M.B. contributed equally to this work.

[2]To whom correspondence may be addressed. E-mail: maya.schuldiner@weizmann.ac.il or Amnon.Horovitz@weizmann.ac.il.

This article contains supporting information online at www.pnas.org/lookup/suppl/doi:10.1073/pnas.1209277109/-/DCSupplemental.

CELL BIOLOGY

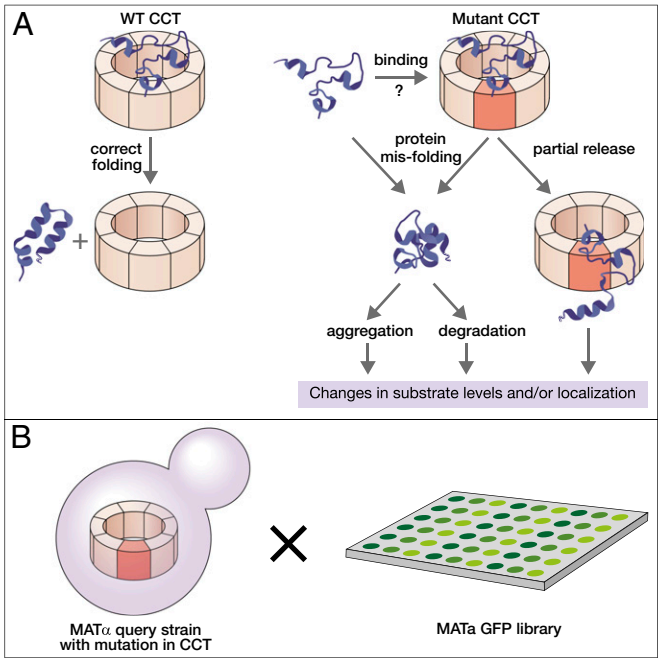

Fig. 1. Scheme showing the approach put forward in this work for screening effects of mutations in CCT on substrate folding and localization. (*A*) The mutation in the ATP binding sites of subunits CCT3 or CCT6 (in red) can interfere with substrate binding and cause misfolding. Substrates can also misfold after binding to the mutant CCT or be released only partially. Misfolding can lead to aggregation or degradation that may be reflected in changes in protein levels and/or localization. (*B*) Strains with the mutation in CCT were crossed with a library of strains expressing endogenous yeast proteins fused to GFP. The resulting strains, each expressing wild-type (control) or mutant CCT and an endogenous yeast protein fused to GFP, were subjected to high-throughput microscopy screening to determine changes in protein levels and localization.

chaperone specificity in an unbiased and system-wide manner can be achieved by adopting the approach used in this study.

Results and Discussion

The *S. cerevisiae* (S288C) Y6545 strains with the mutations D91E and D89E in subunits CCT3 and CCT6, respectively, were generated by homologous recombination as previously described (14). These two query strains with mutations in subunits CCT3 or CCT6 were crossed using the synthetic genetic array (SGA) methodology (15, 19) with a complete library of haploid strains expressing endogenous yeast proteins fused at their C termini to GFP (17), thereby yielding two libraries designated throughout this article as MA3 and MA6, respectively. The libraries of ~5,100 strains, each expressing either wild-type (control) or mutant CCT and an endogenous yeast protein fused to GFP, were subjected to high-throughput microscopy screening to determine changes in protein levels and localization.

Mutations in CCT Lead to a Dramatic Accumulation of P-Bodies. We first analyzed changes in protein localization that occurred in the two mutants strains relative to the wild-type library. Eight proteins (Kem1, Pat1, Nmd4, Nam7, Lsm2, Lsm3, Dcp1, and Dcp2) that are known to be involved in P-body formation (18) were found to form much more prominent puncta in the MA3 strain relative to the wild-type and MA6 strains (Fig. 2*A*). Colocalization experiments with Edc3, a P-body marker, fused to mCherry confirmed that these puncta are indeed P-bodies and not simply aggregates of these P-body proteins caused by their misfolding as a result of the mutation in subunit CCT3 (Fig. 2*B*). The appearance of P-bodies in the MA3 strains could reflect a general response to stress caused by the mutation because it was shown that exposure of *S. cerevisiae* cells to various forms of stress, such as glucose deprivation or hypotonic shock, can cause P-body formation (18). P-body formation can also be stimulated by microtubule disruption (20). Indeed, treating wild-type cells with benomyl (a β-tubulin polymerization inhibitor) and/or latruncilin-A (an actin polymerization inhibitor) was found to cause P-body formation (20). Formation of P-bodies in *S. cerevisiae* can also be induced by overexpression or deletion of some of their key components (18). The latter may occur if the mutation in subunit CCT3 affects the folding of certain P-body components. Interestingly, it was shown that P-body assembly involves glutamine- and/or asparagine-rich (Q/N-rich) regions in some of its components (21). It has also been shown that CCT interacts with the Q/N-rich huntingtin protein that is implicated in Huntington's disease (22–24). Hence, we decided to examine whether P-body formation in the MA3 strain reflects an interaction of subunit CCT3 with Q/N-rich regions that is absent or weaker in the case of subunit CCT6.

Changes in Protein Levels Indicate a Role of CCT3 in Q/N-Rich Protein Folding. The unique effects of the mutations were next characterized by examining the changes they caused in protein abundance. We found that each of the mutations affected the levels of several tens of proteins. For example, 46 and 18 proteins were found to be respectively up- and down-regulated significantly ($P < 0.01$) in the MA3 vs. wild-type strain (Dataset S1). A plot of the fold changes in protein levels in MA6 against the fold changes of the corresponding proteins in MA3 (Fig. 3*A*) revealed that three of the nine proteins that change most in MA3 but significantly less in MA6 (Pub1, New1, and Dbp2) are Q/N-rich and involved in P-body formation. This finding prompted us to examine whether the fold changes in levels of Q/N-rich proteins are, in general, larger in their absolute values in MA3 relative to MA6. We therefore calculated the SDs of the fold change values in MA3 and MA6 for the list of yeast Q/N-rich proteins [compiled previously (25)] and compared them with the SDs of many groups of the same size that contain randomly selected proteins that are not included in the list of Q/N-rich proteins. It may be seen in Fig. 3*B* that the SD of the fold change values of the Q/N-rich proteins in MA3 is significantly larger than those of the groups of randomly selected proteins in MA3 that are not Q/N-rich. By contrast, the SD of the fold change values of the Q/N-rich proteins (25) in MA6 is only marginally larger than those of the groups of randomly selected proteins (Fig. 3*B*). These results indicate that the levels of Q/N-rich proteins are affected (decreased or increased) more by the mutation in subunit CCT3 than by the corresponding mutation in subunit CCT6.

Given that changes in protein levels can be due to a direct interaction with the mutated subunit or to an indirect cellular cause, we next asked whether the proteins (including those that are not Q/N-rich) whose levels are found to change significantly in MA3 but not MA6 (Fig. 3*A*) have more interactions with Q/N-rich proteins than randomly chosen proteins. We found that eight of these nine proteins have at least one physical or genetic interaction with Q/N-rich proteins, whereas in randomly chosen groups of nine proteins a significantly smaller number of only four to five proteins, on average, have physical or genetic interactions with Q/N-rich proteins (Fig. 3*C*). Taken together, these results and those in Fig. 3*B* led us to hypothesize that subunit CCT3 has a specialized role in folding Q/N-rich proteins.

Structural Modeling Reveals a Potential Binding Site in Subunit CCT3 for Q/N-Rich Regions. Given the above-described evidence obtained from the high-throughput microscopy screening approach for the interaction of subunit CCT3 with Q/N-rich proteins, we next asked whether there is any structural evidence for such an interaction. Structural data for the entire CCT complex is currently available only at 3.8-Å resolution (10), but fortunately the crystal

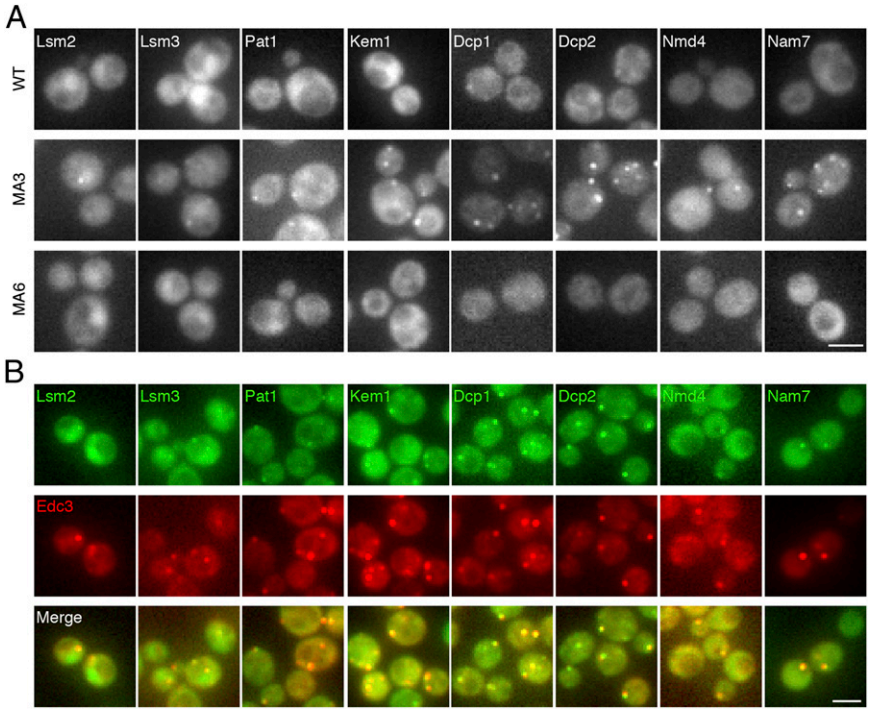

Fig. 2. P-bodies are formed in strains with the mutation in the ATP binding site of subunit CCT3. (*A*) P-body proteins (Lsm2, Lsm3, Pat1, Kem1, Dcp1, Dcp2, Nmd4, and Nam7) form much more pronounced puncta in the MA3 strain relative to the MA6 and wild-type strains. (*B*) Colocalization experiments were carried out by transforming the strains in *A* with a plasmid expressing the P-body marker, Edc3-mCherry. A perfect merge between the GFP-tagged P-body proteins and the Edc3-mCherry protein is observed, indicating that the puncta are bona fide P-bodies. (Scale bars, 5 μm.)

structure of the apical domain of subunit CCT3 from mouse has been solved at 2.2-Å resolution (26). This structure, as well as that of the apical domain of GroEL (27) as a control, were analyzed using an algorithm that detects energetically favorable anchoring spots for amino acid side chains on protein surfaces (28). The analysis shows that the apical domain of GroEL contains relatively few Q/N anchoring spots and that most of them are not located in the substrate binding area (Fig. 4). By contrast, the apical domain of subunit CCT3 is found to contain a large number of Q/N anchoring spots, many of which are located in the probable substrate binding area. The number of anchors with $\Delta G < -4$ kcal/mol and within 3.5 Å from any of the substrate binding site atoms is 2.6-fold greater in CCT3 than in GroEL after normalizing for the accessible surface areas of their respective substrate binding sites. Particularly remarkable is the observation that the spacing of six of the anchoring spots in the substrate binding area of subunit CCT3 is ideal for binding a Q/N-rich segment in a regular β-strand conformation (Fig. 4).

Given the model of a binding site in CCT3 for a Q/N-rich segment (Fig. 4), we sought to uncover the entire set of yeast proteins that have the potential to bind directly to the anchoring spots in our predicted CCT3 binding surface. To this end, a comprehensive scan of the 6,583 yeast proteins found in the UniProt database was performed for segments of seven residues that contain five or more Q/N. Overall, 737 proteins were found to contain such segments. Of the 27 proteins in the MA3 strain that aggregate or whose levels increase or decrease by a factor of at least two, six were found to contain at least one such Q/N-rich segment (*P* value 0.025, Fischer exact test) (Fig. 5). By contrast, only one of the 26 proteins, New1, which changed in the MA6 strain, was found to contain such a segment (*P* value 0.8, Fischer exact test) (Fig. 5). However, New1 was also found to change in MA3, thus indicating a more general explanation for this change.

In Vitro Binding Assays Demonstrate the Importance of Subunit CCT3 in Binding Q/N-Rich Regions. To further test whether subunit CCT3 interacts with Q/N-rich regions, we established an in vitro native gel-shift assay for the binding of CCT to aggregates of Q/N-rich proteins. Using this assay, we characterized the binding of purified CCT complexes to aggregates of Lsm4-EYFP, a Q/N-rich protein that is involved in P-body formation. Wild-type CCT was found to have the highest affinity for these aggregates, followed by CCT(CCT6$_{D89E}$) and then CCT(CCT3$_{D91E}$) that has the lowest affinity (Fig. 6). The lower affinity for the aggregates of subunits CCT3 and CCT6 with the mutations may be due to the larger fraction of time they spend in an ATP-bound state. Strikingly, the rank order of affinities found in the in vitro assays mirrors the stronger interaction in vivo with Q/N-rich proteins of CCT3 compared with CCT6 found using the high-throughput microscopy screening.

Conclusions

In this study we have shown, using high-throughput microscopy screening, that subunit CCT3 has a stronger interaction in vivo with Q/N-rich proteins than subunit CCT6. Our results do not rule out, however, the interaction of other CCT subunits, such as CCT1 (22), with Q/N-rich proteins, and they also do not imply that CCT3 is involved in the folding of Q/N-rich proteins only. A subset of Q/N-rich proteins involved in mRNA decay seems to be particularly affected by the mutation in subunit CCT3 (Figs. 2 and 5), although many other Q/N-rich proteins are also affected (Fig. 3*B*). Given that P-body formation can be induced by depletion of one of its components (18), the link between P-body formation and CCT that is found here might be due to misfolding of a CCT3-dependent substrate (e.g., Pub1 whose level in MA3 is found to be lower than in wild-type by a factor of ~10). Our experimental findings are supported by a computational structural analysis of the apical domain of CCT3 that revealed a putative binding site for six Q/Ns in a β-strand conformation (Fig.

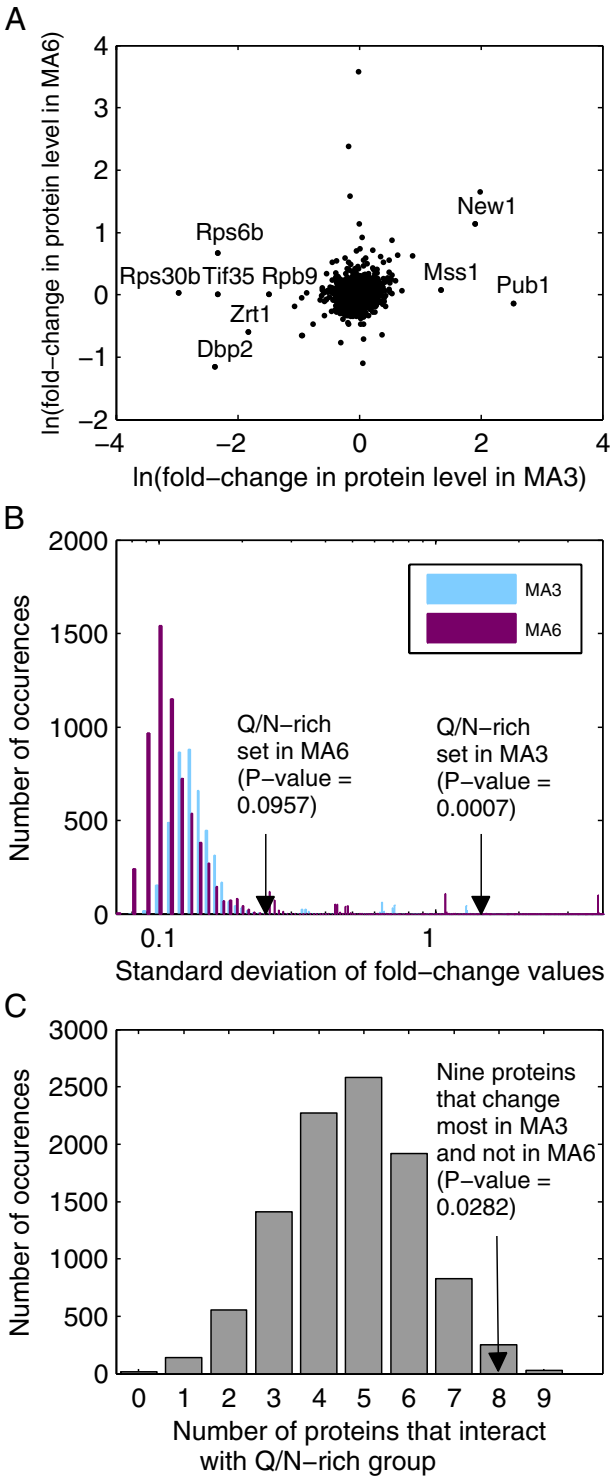

Fig. 3. Levels of Q/N-rich proteins and their interaction partners change more in MA3 than in MA6 cells. (*A*) The natural logarithms of the fold change values of protein levels in MA6 are plotted against those of the corresponding proteins in MA3. The proteins whose levels in MA3 increase or decrease by a factor of 3 or more (relative to wild-type) and in MA6 by a factor of less than 3 (relative to MA3) are designated. (*B*) The SDs of the fold change values for the list of Q/N-rich proteins (compiled in ref. 25) are calculated for MA3 and MA6 (arrows) and compared with the SDs of 10^4 groups of the same size that contain randomly selected proteins that are not included in the list of Q/N-rich proteins. (*C*) Eight of the nine proteins in *A* are found to have at least one physical or genetic interaction with Q/N-rich proteins (arrow), whereas in randomly chosen groups of nine proteins only four to five proteins, on average, have physical or genetic interactions with Q/N-rich proteins.

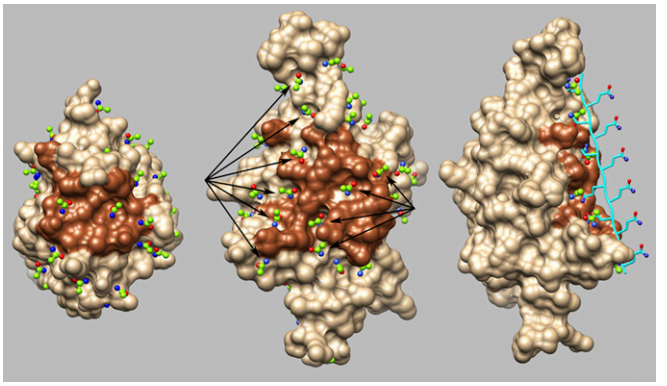

Fig. 4. Mapping of anchoring spots for Q/N on the surfaces of the apical domain of GroEL (*Left*) and CCT3 (*Center* and *Right*). The solvent accessible surfaces of the apical domains of CCT3 (26) and GroEL (27) are shown with the substrate binding sites highlighted in brown. The terminal $CH_2CO(NH_2)$ groups of the anchors with $\Delta G \leq -4$ kcal/mol are shown, with the C, N and O atoms in green, blue, and red, respectively. Arrows in *Center* highlight two stretches of approximately equally spaced anchors. (*Right*) A model of a poly-Q β-strand bound to CCT3 and occupying the long stretch of anchoring sites. Figure prepared with Chimera software (33, 34).

4). Such a Q/N binding site is not observed in the apical domain of GroEL that is also found to contain much fewer anchoring spots for Q/N. This structural difference between the apical domains of CCT3 and GroEL may reflect the fact that eukaryotes (including yeast) contain more Q/N-rich proteins than mesophilic bacteria such as *E. coli* (Fig. 7 and ref. 25). Consequently, it is not surprising that binding sites for Q/N-rich segments have evolved in eukaryotic but not prokaryotic chaperonins. We anticipate that using the approach outlined here for high-content screening of genetically engineered libraries will facilitate elucidating the specificities of other cellular folding machineries and their components.

Methods

Synthetic Genetic Arrays. The *S. cerevisiae* (S288C) Y6545 strain was used to build the SGA query strains (*Δhis3 Δleu2, lys2+Δmet15, Δura3, Δcan:MFA1pr-leu2, Δlyp1, cyh2*, Tef2pr-mCherry::URA*)* with the mutations D91E and D89E in subunits CCT3 and CCT6, respectively. Introduction of the mutations in CCT3 and CCT6 was performed by homologous recombination as previously

Fig. 5. Graphical representation of the most Q/N-rich segments of seven residues in the proteins that aggregate or whose levels increase or decrease by a factor of two in the MA3 and MA6 strains. Light gray, dark gray, and black designate Q, N, and all other residues, respectively.

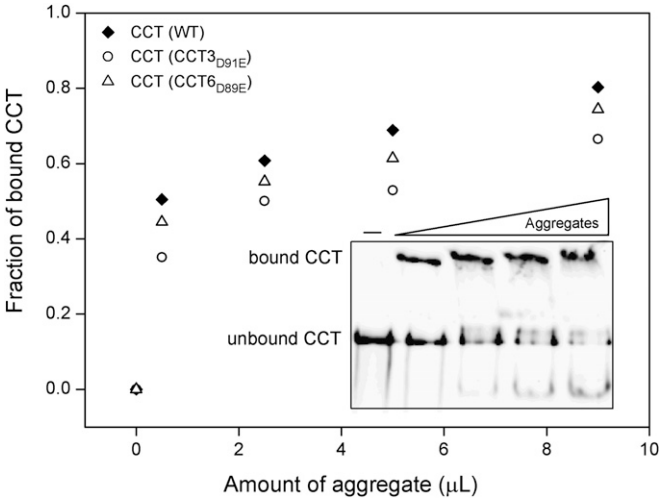

Fig. 6. Plot of fraction of aggregate-bound CCT as a function of amount of aggregate added. Equal concentrations of wild-type or mutant CCT were added to increasing amounts of cell extract containing aggregates of Lsm4-EYFP. The ratio of [bound CCT]/[total CCT] is plotted against the amount of aggregate added. (*Inset*) Result of a representative Western blot in the case of CCT with the mutation in CCT6.

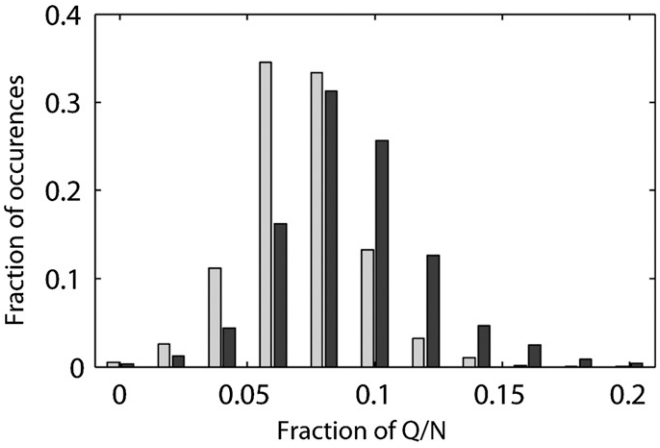

Fig. 7. Q/N-rich proteins are more common in yeast than in *E. coli*. The histogram shows the frequencies of proteins in yeast (dark gray) and *E. coli* (light gray) with different fractions of Q/N (the number of Q/N residues in a protein divided by its total number of residues). The sequences were taken from UniProt.

described (14), and the resulting strains are designated here as MA3 and MA6. A library of haploid *S. cerevisiae* strains, each expressing an endogenous locus yeast protein tagged in-frame at its C terminus to GFP (17), was crossed with these MA3 and MA6 query strains. These diploid strains were subjected to sporulation and selection on SD (– arg, – lys, – ura, – leu, – his, + S-AEC, + canavanine, + G418) plates for haploid strains that carry the mutation in CCT and express a given GFP-tagged protein. *SI Methods* provides more details.

High-Throughput Fluorescence Microscopy. Microscopic screening was performed using an automated microscopy setup as previously described (15). Cells were moved from agar plates into liquid in 384-well polystyrene growth plates using the RoTor arrayer. Liquid cultures were grown overnight in SD medium in a shaking incubator (LiCONiC Instruments) at 30 °C. A JANUS liquid handler (Perkin-Elmer), which is connected to the incubator, was used to back-dilute the strains to ~0.25 OD into plates containing the same medium, after which plates were transferred back to the incubator and the cells were allowed to grow for 3.5 h at 30 °C to reach logarithmic growth phase, as was validated in preliminary calibration. The liquid handler was then used to transfer strains into glass-bottom 384-well microscope plates (Matrical Bioscience) coated with Con A (Sigma-Aldrich) to allow cell adhesion. Wells were washed twice in medium to remove unconnected cells and reach cell monolayers. Plates were then transferred into an automated inverted fluorescent microscopic ScanR system (Olympus) using a swap robotic arm (Hamilton). The ScanR system is designed to allow auto focus and imaging of plates in 384-well format using a 60× air lens and is equipped with a cooled CCD camera. Images were acquired using GFP (excitation at 490 ± 20 nm, emission at 535 ± 50 nm) and mCherry (excitation at 572 ± 35 nm, emission at 632 ± 60 nm) channels. The images were preprocessed by background subtraction and segmentation into single-cell objects on the basis of the cytosolic mCherry expression. GFP intensity was extracted and defined per each object. More details regarding image analysis and data processing are given in *SI Methods*.

Gel-Shift Assays. Equal amounts (2 μg) of wild-type or mutant CCT complexes that were purified as before (29) were mixed with increasing amounts of extract containing aggregates of Lsm4 fused to EYFP obtained from cells harboring the pAG424GAL expression plasmid of this protein (30, 31). The reaction mixtures were incubated for 5 min on ice and then separated by native gel electrophoresis. The amounts of free and aggregate-bound CCT were determined by Western blotting using a mouse monoclonal anti-polyHistidine peroxidase antibody. More details are given in *SI Methods*.

Mapping Anchoring Spots. ANCHORSMAP (28) was used to detect preferred binding locations of Asn and Gln residues on the surfaces of the apical domains of CCT3 [Protein Data Bank (PDB) code 1gml] and GroEL (PDB code 1kid). ANCHORSMAP detects surface cavities adequate for binding single amino acid side chains, scatters thousands of excised amino acid probes in the vicinity of these cavities, optimizes their positions, and accurately estimates the ΔG of binding, taking into consideration that the amino acid is part of a hypothetical protein. Anchoring spots with $\Delta G \leq -4$ kcal/mol were considered in subsequent analyses because such low energy anchoring spots were found to often correspond to experimentally detected hot spots (28). Solvent accessibility was calculated with NACCESS v2.1 (32).

ACKNOWLEDGMENTS. We thank Dr. Simon Alberti for the collection of plasmids expressing Q/N-rich proteins fused to EYFP and Dr. Roy Parker for the Edc3-mCherry plasmid. This work was supported by the Kahn Center for Systems Biology grant (to M.B.) and by ERC-StG-2010 260395 - ER Architecture (to M.B. and M.S.) and by Grant 153/08 of the Israel Science Foundation (to A.H.). Part of this work was carried out while K.R.W. was a Weston Visiting Professor at the Weizmann Institute. A.H. is an incumbent of the Carl and Dorothy Bennett Professorial Chair in Biochemistry.

1. Horwich AL, Fenton WA, Chapman E, Farr GW (2007) Two families of chaperonin: physiology and mechanism. *Annu Rev Cell Dev Biol* 23:115–145.
2. Yébenes H, Mesa P, Muñoz IG, Montoya G, Valpuesta JM (2011) Chaperonins: two rings for folding. *Trends Biochem Sci* 36(8):424–432.
3. Azia A, Unger R, Horovitz A (2012) What distinguishes GroEL substrates from other *Escherichia coli* proteins? *FEBS J* 279(4):543–550.
4. Gao Y, Thomas JO, Chow RL, Lee GH, Cowan NJ (1992) A cytoplasmic chaperonin that catalyzes β-actin folding. *Cell* 69(6):1043–1050.
5. Yaffe MB, et al. (1992) TCP1 complex is a molecular chaperone in tubulin biogenesis. *Nature* 358(6383):245–248.
6. Dekker C, et al. (2008) The interaction network of the chaperonin CCT. *EMBO J* 27(13):1827–1839.
7. Yam AY, et al. (2008) Defining the TRiC/CCT interactome links chaperonin function to stabilization of newly made proteins with complex topologies. *Nat Struct Mol Biol* 15(12):1255–1262.
8. Gong Y, et al. (2009) An atlas of chaperone-protein interactions in *Saccharomyces cerevisiae*: implications to protein folding pathways in the cell. *Mol Syst Biol* 5:275.
9. Kalisman N, Adams CM, Levitt M (2012) Subunit order of eukaryotic TRiC/CCT chaperonin by cross-linking, mass spectrometry, and combinatorial homology modeling. *Proc Natl Acad Sci USA* 109(8):2884–2889.
10. Dekker C, et al. (2011) The crystal structure of yeast CCT reveals intrinsic asymmetry of eukaryotic cytosolic chaperonins. *EMBO J* 30(15):3078–3090.
11. Llorca O, et al. (1999) Eukaryotic type II chaperonin CCT interacts with actin through specific subunits. *Nature* 402(6762):693–696.
12. Rivenzon-Segal D, Wolf SG, Shimon L, Willison KR, Horovitz A (2005) Sequential ATP-induced allosteric transitions of the cytoplasmic chaperonin containing TCP-1 revealed by EM analysis. *Nat Struct Mol Biol* 12(3):233–237.
13. Horovitz A, Willison KR (2005) Allosteric regulation of chaperonins. *Curr Opin Struct Biol* 15(6):646–651.

14. Amit M, et al. (2010) Equivalent mutations in the eight subunits of the chaperonin CCT produce dramatically different cellular and gene expression phenotypes. *J Mol Biol* 401(3):532–543.
15. Cohen Y, Schuldiner M (2011) Advanced methods for high-throughput microscopy screening of genetically modified yeast libraries. *Methods Mol Biol* 781:127–159.
16. Vizeacoumar FJ, Chong Y, Boone C, Andrews BJ (2009) A picture is worth a thousand words: genomics to phenomics in the yeast *Saccharomyces cerevisiae*. *FEBS Lett* 583 (11):1656–1661.
17. Huh WK, et al. (2003) Global analysis of protein localization in budding yeast. *Nature* 425(6959):686–691.
18. Eulalio A, Behm-Ansmant I, Izaurralde E (2007) P bodies: at the crossroads of post-transcriptional pathways. *Nat Rev Mol Cell Biol* 8(1):9–22.
19. Tong AH, et al. (2001) Systematic genetic analysis with ordered arrays of yeast deletion mutants. *Science* 294(5550):2364–2368.
20. Sweet TJ, Boyer B, Hu W, Baker KE, Coller J (2007) Microtubule disruption stimulates P-body formation. *RNA* 13(4):493–502.
21. Reijns MA, Alexander RD, Spiller MP, Beggs JD (2008) A role for Q/N-rich aggregation-prone regions in P-body localization. *J Cell Sci* 121(Pt 15):2463–2472.
22. Tam S, Geller R, Spiess C, Frydman J (2006) The chaperonin TRiC controls polyglutamine aggregation and toxicity through subunit-specific interactions. *Nat Cell Biol* 8(10):1155–1162.
23. Kitamura A, et al. (2006) Cytosolic chaperonin prevents polyglutamine toxicity with altering the aggregation state. *Nat Cell Biol* 8(10):1163–1169.
24. Behrends C, et al. (2006) Chaperonin TRiC promotes the assembly of polyQ expansion proteins into nontoxic oligomers. *Mol Cell* 23(6):887–897.
25. Michelitsch MD, Weissman JS (2000) A census of glutamine/asparagine-rich regions: implications for their conserved function and the prediction of novel prions. *Proc Natl Acad Sci USA* 97(22):11910–11915.
26. Pappenberger G, et al. (2002) Crystal structure of the CCTγ apical domain: implications for substrate binding to the eukaryotic cytosolic chaperonin. *J Mol Biol* 318(5):1367–1379.
27. Buckle AM, Zahn R, Fersht AR (1997) A structural model for GroEL-polypeptide recognition. *Proc Natl Acad Sci USA* 94(8):3571–3575.
28. Ben-Shimon A, Eisenstein M (2010) Computational mapping of anchoring spots on protein surfaces. *J Mol Biol* 402(1):259–277.
29. Shimon L, Hynes GM, McCormack EA, Willison KR, Horovitz A (2008) ATP-induced allostery in the eukaryotic chaperonin CCT is abolished by the mutation G345D in CCT4 that renders yeast temperature-sensitive for growth. *J Mol Biol* 377(2): 469–477.
30. Alberti S, Gitler AD, Lindquist S (2007) A suite of Gateway cloning vectors for high-throughput genetic analysis in *Saccharomyces cerevisiae*. *Yeast* 24(10):913–919.
31. Alberti S, Halfmann R, King O, Kapila A, Lindquist S (2009) A systematic survey identifies prions and illuminates sequence features of prionogenic proteins. *Cell* 137 (1):146–158.
32. Hubbard SJ, Thornton JM (1993) *NACCESS Computer Program* (University College London, London).
33. Pettersen EF, et al. (2004) UCSF Chimera—a visualization system for exploratory research and analysis. *J Comput Chem* 25(13):1605–1612.
34. Sanner MF, Olson AJ, Spehner JC (1996) Reduced surface: an efficient way to compute molecular surfaces. *Biopolymers* 38(3):305–320.